J. Membrane Biol. 150, 63–71 (1996)

The Journal of
Membrane
Biology

Calcium-dependent Enhancement of Depletion-activated Calcium Current in Jurkat T Lymphocytes

E.P. Christian, K.T. Spence, J.A. Togo, P.G. Dargis, J. Patel
Department of Pharmacology, Zeneca Pharmaceuticals, 1800 Concord Pike, Wilmington, DE 19850

Received: 30 August 1995/Revised: 7 November 1995

Abstract. We have obtained evidence that the Ca^{2+}-selective current activated by Ca^{2+} store depletion (Ca^{2+} release-activated Ca^{2+} current; I_{crac}) in Jurkat T lymphocytes is augmented in a time-dependent manner by Ca^{2+} itself. Whole cell patch clamp experiments employed high cytosolic Ca^{2+}-buffering conditions to passively deplete Ca^{2+} stores. Rapidly switching to nominally Ca^{2+}-free extracellular buffer instantaneously reduced I_{crac} measured at −100 mV to leak current level. Unexpectedly, readmission of 2 mM Ca^{2+} instantaneously restored only 38 ± 5% (mean ± SEM; n = 9) of the full I_{crac} amplitude. The remainder reappeared in a monotonic time-dependent manner over 10 to 20 sec. Rapid *vs.* slow intracellular Ca^{2+} chelators did not alter this process, and inorganic I_{crac} blockers did not regenerate it, arguing against an intracellular site of action. The effect was specific to Ca^{2+}: introduction of the permeant ions, Ba^{2+} or Sr^{2+}, failed to invoke time-dependent I_{crac} reappearance. Moreover, equimolar substitution of Ba^{2+} for Ca^{2+} initially produced Ba^{2+} current of similar magnitude to the full Ca^{2+} current, but the Ba^{2+} current decayed monotonically to <50% of its initial amplitude in <20 sec. Conversely, return to Ca^{2+} produced a time-dependent increase in I_{crac} to its larger Ca^{2+} permeation level. Thus Ca^{2+} appears to selectively promote a reversible transition of I_{crac} that results in larger current flux, and at least partially explains the selectivity of this current for Ca^{2+} over other divalent ions.

Key words: Ca^{2+} current — Depletion-activated Ca^{2+} current — Voltage-independent Ca^{2+} current — Ca^{2+} selectivity — Ba^{2+} permeation — Jurkat cell

Correspondence to: E.P. Christian

Introduction

Plasma membrane Ca^{2+} channels coupled to the depletion of Ca^{2+} from microsomal stores have been pursued enthusiastically by investigators in recent years. None of these channels have been cloned with the possible exception of an insect homolog, *trp,* from Drosophila (Hardie & Minke, 1993; Vaca et al., 1994). Thus no definitive information is available about the degree of structural homology among depletion-activated Ca^{2+} channels. Nonetheless, the biophysical properties and biochemical regulation of these channels appear to be increasingly diverse, suggesting that they may comprise an extensive family of molecular entities. Some of the most detailed biophysical analyses of depletion-activated Ca^{2+} channel characteristics have emerged from whole cell patch clamp studies in mast cells (Hoth & Penner, 1992, 1993; Hoth, 1995) and cultured Jurkat T lymphocytes (Lewis & Cahalan, 1989; McDonald, Premack & Gardner, 1993; Zweifach & Lewis, 1993, 1995; Premack, McDonald & Gardner, 1994; Hoth, 1995). These hallmark properties include: strong Ca^{2+} selectivity, greater Ca^{2+} than Ba^{2+} permeation, time and voltage-independent gating, inward rectification at negative potentials, and Ca^{2+}-dependent rapid inactivation. In mast cells the depletion-activated current was originally referred to as Ca^{2+} release-activated Ca^{2+} current (I_{crac}; Hoth & Penner, 1992), and this naming convention was subsequently adopted in T cells (Zweifach & Lewis, 1995). Single channel currents corresponding to I_{crac} have not been recorded successfully in these cells. However, estimates from noise analysis in Jurkat cells suggest exceedingly low unitary conductance in the fS range (Zweifach & Lewis, 1993). This contrasts to Ca^{2+}-selective single channels that have been recorded in several cell types with apparent Ca^{2+} store-dependent linking, but unitary conductances in the pS range (Lückhoff & Chapham, 1994; Vaca & Kunze, 1994).

The primary defining criterion of depletion-

activated Ca^{2+} currents is the coupling of activation to the Ca^{2+} status of intracellular stores. Yet, regulation of open probability of these channels appears complex. Although considerable attention has been directed toward elucidating the coupling pathway between Ca^{2+} store depletion and Ca^{2+} current activation, mechanisms unrelated to store depletion have also been shown to modulate depletion-activated currents. Rapid (τ < 150 msec) Ca^{2+}-dependent inactivation of I_{crac} in mast cells (Hoth & Penner, 1993) and Jurkat T cells (Zweifach & Lewis, 1995), similar to that shown in voltage-gated Ca^{2+} channels (Chad & Eckert, 1984), provides one example of this: recent evidence indicates that this fast inactivation may result from a direct interaction of Ca^{2+} near the inner aspect of the I_{crac} channel pore (Zweifach & Lewis, 1995). Whether this property generalizes to other depletion-activated Ca^{2+} currents remains to be determined.

In the present study, we have identified a second Ca^{2+}-dependent regulatory effect on I_{crac} in Jurkat cells whereby introduction of extracellular Ca^{2+} itself directly *augments* the whole cell current. This effect is not mimicked by other permeant divalent ions such as Ba^{2+} and Sr^{2+}. Thus Ca^{2+} seems to be unique as a charge carrier that promotes a transition of I_{crac} channels to achieve maximal Ca^{2+} influx for a given level of store depletion. These findings may provide new insights into mechanisms underlying the high Ca^{2+} selectivity of I_{crac}. Importantly, our findings also impart a further characteristic to the biophysical signature of the T cell I_{crac} for comparison to other depletion-activated Ca^{2+} currents.

Materials and Methods

Cell Culture

Studies were performed on human leukemic E6-1 Jurkat cells. Cell cultures were maintained at log phase growth between 0.1 and 1.5×10^6 cells/ml in medium containing RPMI 1640 (Mediatech, Herndon, VA) and 10% Fetal Bovine Serum Defined (HyClone, Logan, UT). Cell cultures were incubated at 37°C in an atmosphere containing 5% CO_2. For recording, cells in a 150 μl aliquot of media were allowed to adhere to a poly-D-lysine-coated plastic culture dish for 3–5 min.

Whole-cell Recording

All constituents for solutions were purchased from Sigma (St. Louis, MO) except for CsOH (Aldrich, Milwaukee, WI), and Cs_4BAPTA (1,2-Bis(2-aminophenoxy)ethane-*N*,*N*,*N′*,*N′*-tetraacetic acid) (Molecular Probes, Eugene, OR). Standard extracellular recording solution was (in mM): NaCl, 160; KCl, 4.5; $CaCl_2$, 2; $MgCl_2$, 1; D-glucose, 5; HEPES (*N*-2-hydroxyethylpiperazine-*N′*-2-ethanesulfonic acid), 5; pH to 7.4 with NaOH; Standard pipette solution was (in mM): cesium aspartate, 140; $MgCl_2$, 2; EGTA (ethyleneglycol-*bis*-(β-aminoethyl ether)*N*,*N*,*N′*,*N′*-tetraacetic acid), 10; HEPES, 10; pH, 7.2 with CsOH. The pipette solution was hyposmotic (~305 mOsm), relative to the extracellular solution (~320 mOsm). ''Ca^{2+}-free'' extracellular solution contained nominal free Ca^{2+} (no added Ca^{2+} chelator), and the total divalent ion concentration was made equimolar to the Ca^{2+}-containing solution by Mg^{2+} addition. Experiments were conducted at 22–24°C.

The standard whole cell configuration of the patch clamp technique was used for recordings (Hamill et al., 1981). Pipettes were fabricated from thin wall (1.5 mm OD, 1.12 mm ID) borosilicate glass (Worth Precision Instruments, Sarasota, FL) on a Brown-Flaming P-87 Puller (Sutter Instruments, San Rafael, CA), Sylgarded (Dow Corning, Midland, MI), and polished to a DC resistance of 2–8 MΩ when filled with the pipette solution. Membrane currents were amplified with either an Axopatch 1B or 200A amplifier (Axon Instruments, Foster City, CA). Voltage clamp protocols were implemented and data acquisition performed with pClamp 6.0 software (Axon Instruments). The pipette current was nulled prior to forming a seal. Command potentials were not corrected for the ~−10 mV junction potential calculated (Barry & Lynch, 1991) between the standard pipette and bath solutions. This does not impact significantly any of the conclusions reached in the study. The resistance of patch seals was >10 GΩ. Whole cell capacitive transients were nulled with the capacitance compensation circuitry in the amplifier following attainment of the whole cell mode. In most experiments, 70 to 85% of the series resistance (<20 MΩ) was compensated by the amplifier.

Voltage clamp protocols used a holding potential of 0 mV to minimize basal Ca^{2+} influx. This condition allowed stable recordings of I_{crac} for usually >10 min. I_{crac} was measured during voltage steps to −100 mV of varying duration, or 200-msec ramps between −100 and +40 mV. Leak current (measured in nominally Ca^{2+}-free solution, i.e., 2 mM Mg^{2+} substitution) was always manually subtracted from total Ca^{2+} current to analyze quantitatively the Ca^{2+}-selective I_{crac} amplitude. Data were rejected if either leak current measured in Ca^{2+}-free solution or I_{crac} measured in 2 mM Ca^{2+} varied by >20% during an experiment. Leak subtraction circuitry in the amplifier was not used to acquire data and baseline currents were not digitally subtracted from current traces shown in the figures.

Extracellular solutions were exchanged with a linear array of gravity fed glass-lined tubes (100 μm ID; Hewlett Packard, Wilmington, DE) connected to solenoid valves (BME Systems, Baltimore, MD). In some experiments, solenoid activation and deactivation were time locked to voltage clamp protocols by computer control. The tube containing the desired solution was localized <1 cell diameter from a cell prior to activating the solenoid. This system enabled reequilibration of extracellular solutions in <200 msec, based on the time course for removal of Ca^{2+}-selective flux through I_{crac} channels (*see* Results).

Data Analysis

Membrane currents were low-pass filtered with an 8-pole Bessel filter, and digitized as computer files with p-Clamp software and a TL-1 interface (Scientific Solutions, Solon, OH). A full unfiltered record of currents recorded in the experiment was also pulse encoded to VCR tape. Data epochs from these tapes were filtered and redigitized offline for some experiments. p-Clamp software was used to measure current amplitudes, and Origin software (Microcal, Northampton, MA) was used to iteratively fit various functions to the data and to construct figures. Averaged data are expressed as mean ± SEM. For statistical tests $p < 0.05$ was taken to denote a significant effect.

Results

Identification of I_{crac} in Jurkat Cells

Following attainment of the whole cell configuration with control extracellular and intracellular solutions, the

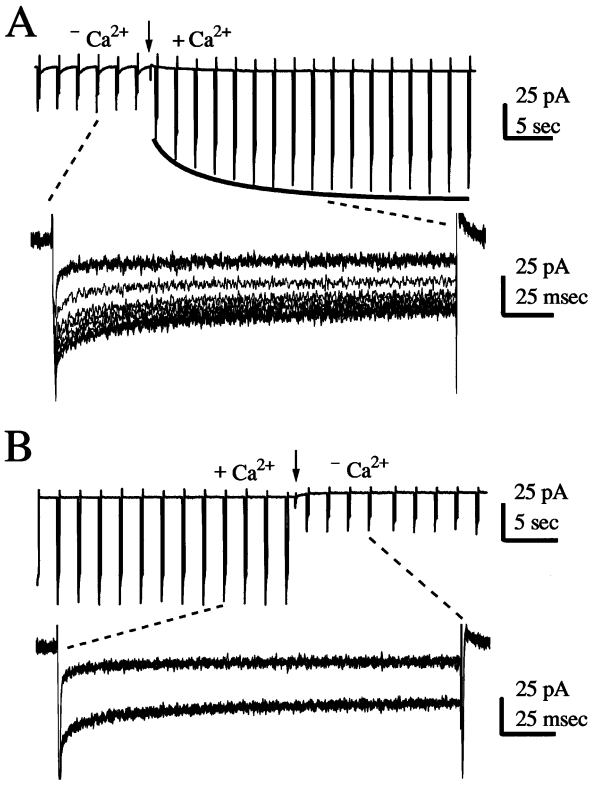

Fig. 1. Time-dependent increase of I_{crac} following Ca^{2+} readmission. Data shown in this and all subsequent figures were obtained after asymptotic I_{crac} development. Inward current is down in all figures. Upper traces in panels *A* and *B* are continuous whole cell current records (filtered at 30 Hz, digitized at 100 Hz) obtained from one cell during reintroduction (+Ca^{2+}; *A*) and removal (–Ca^{2+}; *B*) of 2 mM extracellular Ca^{2+} (arrows denote times of solution exchanges). Voltage clamp protocol delivered a –100 mV, 200 msec step at 0.5 Hz from a 0 mV holding potential. The unbroken line in *A* is a monoexponential function fit to the peak currents recorded during the steps following Ca^{2+} reintroduction ($\tau = 5.1$ sec). Lower traces in *A* and *B* are expanded sweeps of superimposed currents during –100 mV, 200-msec steps taken from the intervals in upper traces denoted by broken lines (data filtered at 1 kHz, digitized at 5 kHz). This format reveals the gradual increase in current during successive voltage steps following replacement of Ca^{2+} (*A*), compared to the discrete change from a high to low amplitude following Ca^{2+} removal (*B*).

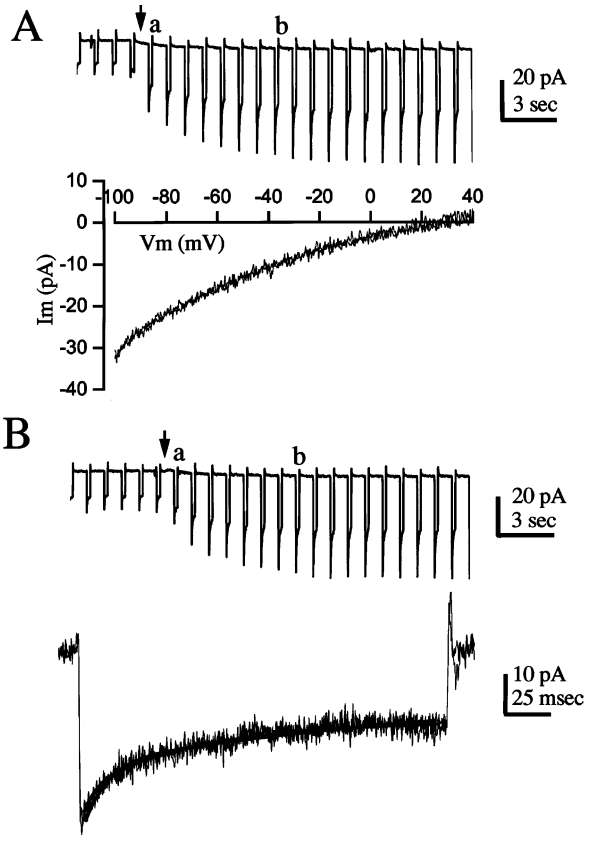

Fig. 2. Invariability of the I_{crac} current-voltage relationship (*A*), and fast inactivation properties (*B*) during Ca^{2+}-dependent increases. Data are from two different cells. (*A*) Upper trace is a continuous whole cell current record (filtered at 30 Hz, digitized at 100 Hz) obtained during readmission of 2 mM Ca^{2+} (arrow). Voltage clamp protocol delivered –100 to +40 mV, 200-msec ramps at 0.5 Hz from a 0 mV holding potential. Lower panel is two superimposed current traces (filtered at 1 kHz, digitized at 5 kHz) obtained during the ramps denoted by points *a* and *b* in the upper trace. Currents are plotted against ramp voltage, and are not baseline leak corrected. The current obtained at *a* was scaled up and superimposed on the current at *b*. (*B*) Upper panel is a continuous current record (filtered at 30 Hz, digitized at 100 Hz) obtained during readmission of 10 mM Ca^{2+} (arrow). The voltage clamp protocol delivered –100 mV, 200-msec steps at 0.5 Hz from a 0 mV holding potential. Lower panel is expanded current traces (filtered at 1 kHz, digitized at 5 kHz) taken during steps at points *a* and *b* in the upper trace. The current obtained at *a* was scaled up and superimposed on that obtained at *b*. Unbroken lines are biexponential fits to the fast inactivation in the two traces (τ values: trace *a:* 8.5 msec, 57 msec; trace *b;* 9.6 msec, 66 msec).

total current monitored by repeated (0.2 to 1 Hz) –100 mV, 200-msec steps from a 0 mV holding potential increased gradually over 2–5 min to an asymptotic level. The time course of this increase was presumed to be coupled to passive store depletion by the strongly Ca^{2+}-buffered pipette solution (i.e., 10 mM EGTA, 0 mM Ca^{2+}; calculated free Ca^{2+} concentration: $<10^{-9}$ M) as it dialyzed the cytosolic compartment. The current recorded during voltage steps or ramps under these conditions (Figs. 1 and 2) exhibited the signature properties documented previously for I_{crac} in Jurkat cells (McDonald et al., 1993; Zweifach & Lewis, 1993; Premack et al., 1994), including low current density (1.31 ± 0.07 pA/pF at –100 mV and 2 mM external Ca^{2+}; $n = 18$), time- and voltage-independent activation, inward rectification at hyperpolarized potentials, and a reversal potential positive to 0 mV. In addition, Ca^{2+} permeation substantially exceeded that of Ba^{2+} (Figs. 4 and 5), and Ni^{2+} and Cd^{2+} produced a rapid current block (Fig. 7). Finally, current decayed with bi-exponential kinetics during a –100 mV, 200-msec step (Fig. 2*B*), reflecting the fast inactivation process which has been described for the mast cell (Hoth

& Penner, 1993), and T cell I_{crac} (Zweifach & Lewis, 1995). Thus I_{crac} recorded under our conditions exhibited an aggregate of characteristics corresponding closely to those documented previously for I_{crac} in T-cells and mast cells.

Ca^{2+}-Mediated Slow Increase in I_{crac} Magnitude

We evaluated the Ca^{2+} dependency of I_{crac} by removal and subsequent replacement of Ca^{2+}-containing extracellular solution. Unexpectedly, the reappearance of steady-state Ca^{2+} current upon Ca^{2+} readmission occurred in a time-dependent manner over 10 to 20 sec (Fig. 1*A*). Current would be predicted to reappear instantaneously, based on the known time- and voltage-independence of I_{crac} activation. Evidence that this slow time-dependent reappearance of I_{crac} did not merely reflect the kinetics of solution exchange was derived from the observation that current rapidly decayed to a minimum level upon removal of Ca^{2+}-containing solutions (Fig. 1*B*). The rapid kinetics of extracellular solution exchange were demonstrated most convincingly in subsequent experiments where Ca^{2+} was removed and current monitored during prolonged voltage steps to −100 mV (Fig. 3). Note that total current in the cell in Fig. 3 (lower panel) decayed to final leak current level within ~200 msec of switching to Ca^{2+}-free solution, a time course typical of all cells studied with this protocol ($n = 7$).

One other plausible explanation for the slow reappearance of whole cell current observed upon readmission of Ca^{2+} is that this time-dependence reflected activation of a composite current, including I_{crac} and other Ca^{2+}-dependent currents. However, two observations argue that the slowly redeveloping current was homogeneous (Fig. 2). First, the *IV* profile of current in response to voltage ramps (Fig. 2*A*), and second, the rate and extent of fast inactivation of current during voltage steps (Fig. 2*B*) both remained constant during reappearance of the current following Ca^{2+} reintroduction. Thus when a smaller current response to a voltage ramp or step obtained immediately following Ca^{2+} readmission was scaled up, it superimposed closely on a larger current response obtained during a ramp or step taken later, after current had regained full amplitude (ramps: $n = 4$, Fig. 2*A;* steps: $n = 6$, Fig. 2*B*). With regard to fast inactivation, no significant difference existed between either the inactivation τs, or the percent of the total current undergoing fast inactivation during a −100 mV, 200-ms-step for the small *vs.* large currents recorded after Ca^{2+} readmission ($n = 6$ experiments; paired *t*-tests).

An experimental protocol was implemented to characterize more quantitatively the time course of I_{crac} reappearance during Ca^{2+} reintroduction by instituting the solution exchange and measuring current continually during a prolonged (25–30 sec) hyperpolarizing step to −100 mV (Figs. 3 and 4). Immediately after the switch to Ca^{2+}-containing solution, a variable component (38 ± 5%; range: 14 to 50% of final current amplitude; $n = 9$) of I_{crac} was restored instantaneously. The remainder reappeared with monoexponential kinetics (τ: 4.13 ± 0.54 sec; range: 2.7 to 5.2 sec; $n = 7$). The boundary between the apparent instantaneous current (i.e., <200 msec after solution exchange) and the time-dependent current was defined by an inflection point, as exemplified in the traces shown on an expanded time base in the lower panels of Fig. 3 (smallest spontaneous component: 14%) and Fig. 4 (largest spontaneous component: 50%).

An effort was made to study the Ca^{2+} concentration-dependence of slow I_{crac} reappearance. Solutions containing 0, 0.5, 2, 10, 20 and 30 mM Ca^{2+} were introduced

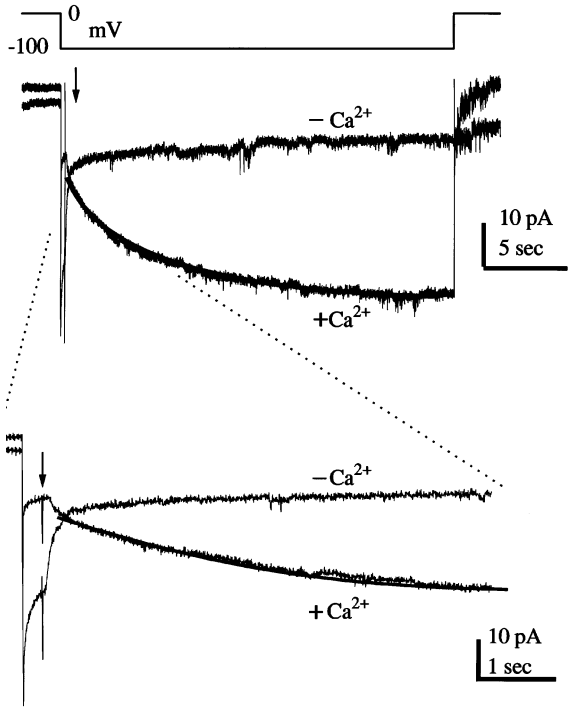

Fig. 3. Kinetics of the Ca^{2+}-dependent I_{crac} increase in a cell. Upper panel is two superimposed whole cell current traces (filtered at 100 Hz, digitized at 500 Hz) obtained during 27-sec voltage steps from 0 to −100 mV (protocol: uppermost trace). Extracellular solution exchanges (*arrow*) were initiated 200 msec after step onset effecting either 2 mM Ca^{2+} removal ($-Ca^{2+}$) or replacement ($+Ca^{2+}$). Lower panel shows portions of sweeps from upper panel on an expanded time base surrounding the voltage step onset and solution exchanges, as denoted by broken lines. I_{crac} declined to an asymptotic level in <200 msec after onset of Ca^{2+} removal. However, as shown by the expanded $+Ca^{2+}$ trace in the lower panel, only a small fraction (~14% at the inflection point) of I_{crac} was restored within 200 msec. The remainder of current redeveloped over ~15 sec with monoexponential kinetics (unbroken line on $+Ca^{2+}$ trace: $\tau = 5.2$ sec).

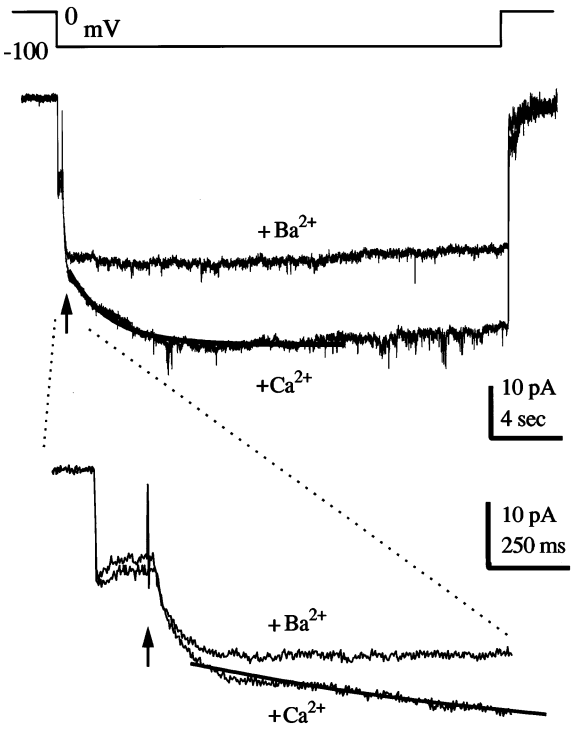

Fig. 4. Selectivity of I_{crac} enhancement for Ca^{2+} over Ba^{2+} in a cell. Voltage clamp protocol and format of figure are identical to Fig. 3, except that extracellular solution exchanges were from Ca^{2+}-free solution to either 2 mM Ca^{2+} ($+Ca^{2+}$) or to 2 mM Ba^{2+} ($+Ba^{2+}$). Addition of Ba^{2+} produced only an apparently instantaneous phase (<200 msec; $+Ba^{2+}$ trace in lower panel) of I_{crac} restoration. By contrast, Ca^{2+} introduction produced an instantaneous component of restoration (lower panel; $+Ca^{2+}$ trace), similar in magnitude to the full Ba^{2+}-mediated current. This was followed by a substantial time-dependent component of current increase that was fitted with a monoexponential function (unbroken line on $+Ca^{2+}$ trace in upper panel; $\tau = 2.7$ sec).

sequentially, while attempting to evaluate the extent and kinetics of slow I_{crac} reappearance at each concentration step jump with −100 mV, 200-msec steps presented at 0.5 Hz ($n = 3$; *data not shown*). A component of slow I_{crac} reappearance was evident at 0.5 mM Ca^{2+} and also for subsequent step jumps through 10 mM Ca^{2+}. Evaluation became impeded at the step jump from 10 to 20 mM Ca^{2+} because of the superimposition of accentuated slow (i.e., seconds time domain) inactivation, coupled with near saturation of conductance through I_{crac}, in agreement with properties which have been documented previously for this current (Hoth & Penner, 1993; McDonald et al., 1993; Zweifach & Lewis, 1993, 1995; Premack et al., 1994). However, in two of the three experiments, slow reappearance was qualitatively evident during the step from 10 to 20 mM Ca^{2+}. Thus the threshold Ca^{2+} concentration for eliciting a slow component of I_{crac} reappearance was below 0.5 mM, and the process did not appear to saturate at a Ca^{2+} concentration below which conductance through I_{crac} saturates.

Ca^{2+} Specificity of I_{crac} Enhancement

We evaluated the Ca^{2+} specificity of slow I_{crac} reappearance by conducting exchange experiments with charge carriers other than Ca^{2+}. I_{crac} in Jurkat cells conducts Ba^{2+} and Sr^{2+} about half as well as Ca^{2+} (McDonald et al., 1993; Zweifach & Lewis, 1993; Premack et al., 1994). Switching from Ca^{2+}-free solution to 2 mM Ba^{2+}-containing solution during a prolonged −100 mV step resulted in the nearly instantaneous (<200 msec) appearance of steady-state Ba^{2+}-mediated I_{crac} (Fig. 4). No time-dependent phase was evident, contrasting to the clear monoexponential increase in current that occurred when switching from Ca^{2+}-free to Ca^{2+}-containing buffer in the same cell (Fig. 4). These data typify the results observed in four experiments, where the steady-state Ba^{2+}-mediated I_{crac} magnitude achieved 46 ± 5% of the full Ca^{2+}-mediated I_{crac} magnitude, in agreement with the known relative permeabilities of these charge carriers. Moreover, in two of these experiments, replacement of 0 mM Ca^{2+} with a 10 mM Ba^{2+}-containing solution also failed to produce any detectable time-dependent component to I_{crac} restoration, although the instantaneously developing current was of larger magnitude than the current in 2 mM Ba^{2+}. Effects analogous to those described for Ba^{2+} were also observed during 2 mM Sr^{2+} introductions ($n = 3$; *data not shown*).

Of particular interest was the finding that the amplitude of the instantaneously restored (i.e., within ~200 msec of exchange) full Ba^{2+}- or Sr^{2+}-mediated I_{crac} was similar in magnitude to the initial instantaneously restored portion of I_{crac} in Ca^{2+} (e.g., Fig. 4). This suggested that the apparent permeation selectivity of I_{crac} for Ca^{2+} over other divalent ions may be actually imparted by the time- and Ca^{2+}-dependent phase of current redevelopment.

Even more compelling evidence that a reversible Ca^{2+}-dependent transition gave rise to the slow I_{crac} increase was derived from experiments where equimolar 2 mM Ca^{2+} and Ba^{2+} solutions were directly interchanged (Fig. 5). When Ca^{2+} was replaced by Ba^{2+} during prolonged −100 mV steps, current first showed a rapid transient decrease over several hundred milliseconds (Fig. 5, lower panel), consistent with an anomalous mole fraction effect (*see* Discussion). Following this transient decrease, the magnitude of Ba^{2+}-mediated I_{crac} magnitude approached that of the full Ca^{2+}-mediated I_{crac} prior to exchange (i.e., mean: 91 ± 2%; range: 84 to 97% of the full Ca^{2+} current amplitude; $n = 5$). The Ba^{2+} current then decayed with monoexponential kinetics (mean τ: 3.52 ± 0.53 sec) to a final level amounting to 41 ± 4% of the initial Ca^{2+}-mediated I_{crac} (Fig. 5, above). Conversely, when the extracellular solution was then switched from Ba^{2+} back to Ca^{2+}, I_{crac} magnitude was initially comparable to the steady-state smaller Ba^{2+} cur-

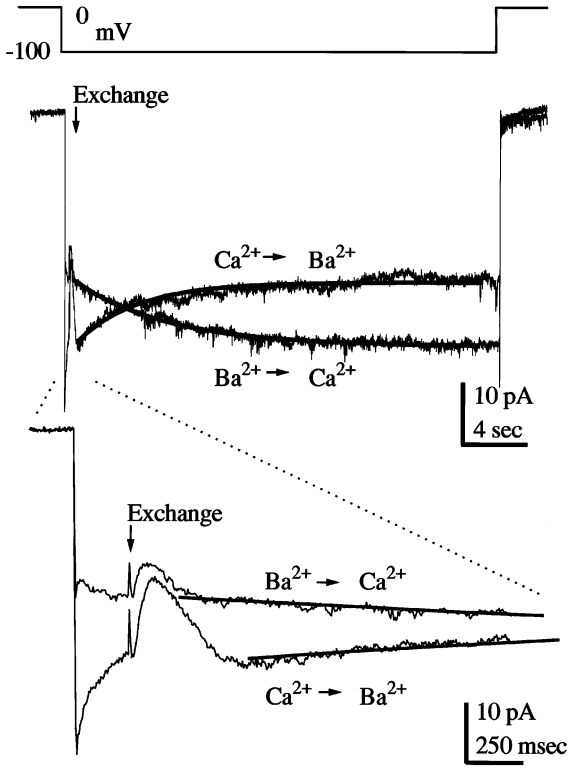

Fig. 5. I_{crac} transitions during exchanges between extracellular Ca^{2+} and Ba^{2+} in a cell. Voltage clamp protocol and format of figure are identical to Fig. 3, except that extracellular solution exchanges were from 2 mM Ca^{2+} to 2 mM Ba^{2+} or *vice versa.* Exchanges initially produced a rapid (<300 msec) transient current minimum (lower panel), likely attributable to an anomalous mole fraction effect (*see* text). Following this effect, Ba^{2+}-mediated current decayed monoexponentially (upper trace; solid line: $\tau = 4.4$ sec) to a lower steady-state Ba^{2+} permeation level, while current in Ca^{2+} increased monotonically ($\tau = 4.7$ sec) to a maximal steady-state Ca^{2+} permeation level.

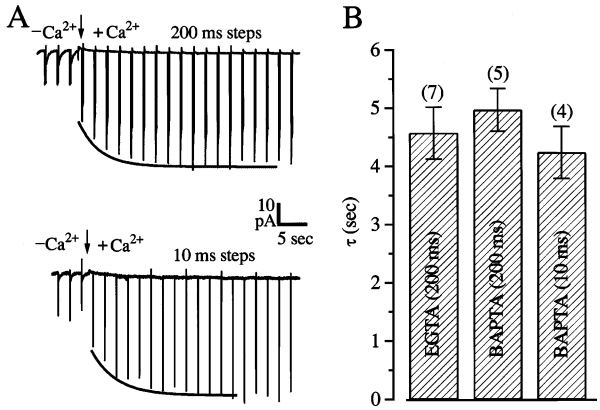

Fig. 6. Effect of different intracellular exogenous Ca^{2+} buffering species on the kinetics of Ca^{2+}-mediated I_{crac} enhancement. (*A*) Time course of I_{crac} enhancement in a cell dialyzed with intracellular solution containing 10 mM BAPTA. Whole cell currents (filtered at 200 Hz; digitized at 500 Hz) were recorded during a voltage clamp protocol that delivered −100 mV, 200-msec (upper panel) or 10-msec (lower panel) steps at 0.5 Hz from a 0 mV holding potential. Solution exchanges (arrows) replaced Ca^{2+}-free buffer with 2 mM Ca^{2+}-containing extracellular buffer. Unbroken lines represent monoexponential fits (τ values: upper panel: 3.94 sec; lower panel: 3.97 sec) to peak currents recorded during steps immediately following Ca^{2+} addition. (*B*) Summary data of effects of intracellular buffers containing either 10 mM EGTA (200-msec steps) or 10 mM BAPTA (200-msec or 10-msec steps) on the kinetics of the Ca^{2+}-dependent I_{crac} increase. Data were obtained from the three experimental treatments (*N*s in parentheses) using the voltage protocols in *A.* Bars show mean ± SEM τ values obtained under each experimental condition. The mean values did not differ significantly between BAPTA- and EGTA-loaded cells (200-msec steps), or between cells loaded with BAPTA and tested with 200-msec versus 10-msec steps (unpaired *t*-tests).

rent, but then monotonically increased over several seconds to its larger final Ca^{2+} permeation level. Thus the Ca^{2+}-Ba^{2+} interchange experiments: (i) directly demonstrated forward and reverse slow transitions of I_{crac} between states supporting higher and lower current flux; (ii) showed that the transition leading to larger current is selectively favored by Ca^{2+} over Ba^{2+}, and (iii) supported further that the permeation selectivity for Ca^{2+} over Ba^{2+} may be conferred by a functional transition of I_{crac} channels, rather than intrinsic pore selectivity.

Site of Ca^{2+} Action

To evaluate whether Ca^{2+} mediated the slow increase in I_{crac} from an intracellular site, the effect was compared in cells dialyzed with either 10 mM EGTA or 10 mM BAPTA, using −100 mV, 200-msec steps presented at 0.5 Hz to measure current. To further limit the extent of Ca^{2+} influx in BAPTA-loaded cells, a second protocol using very brief 10-msec steps (0.5 Hz) was also implemented. A time-dependent phase of I_{crac} restoration was observed during Ca^{2+} readdition under all conditions (Fig. 6). The kinetics (τ values) of Ca^{2+}-dependent I_{crac} reappearance did not differ significantly in the EGTA-*vs.* BAPTA-loaded cells for the 200-msec steps, and also did not differ for the 10-msec *vs.* 200-ms steps in BAPTA-dialyzed cells (Fig. 6*B*). Thus using cytosolic Ca^{2+} buffers with widely different association rates or varying the amount of Ca^{2+} influx via the voltage protocol did not affect quantitatively the kinetics of the Ca^{2+}-dependent I_{crac} increase. These findings provided evidence against Ca^{2+} acting at an intracellular site or biochemical pathway to enhance I_{crac}. The rapid intracellular buffering of Ca^{2+} afforded by 10-mM BAPTA also supported strongly that changes in store depletion status and consequent downstream effects on I_{crac} activation did not account for the Ca^{2+}-dependent I_{crac} increase.

A final set of experiments evaluated the site of Ca^{2+} action by examining the effects of reversibly blocking I_{crac} with the transition metals, Ni^{2+} and Cd^{2+} in the presence of Ca^{2+} (Zweifach & Lewis, 1993; Premack et

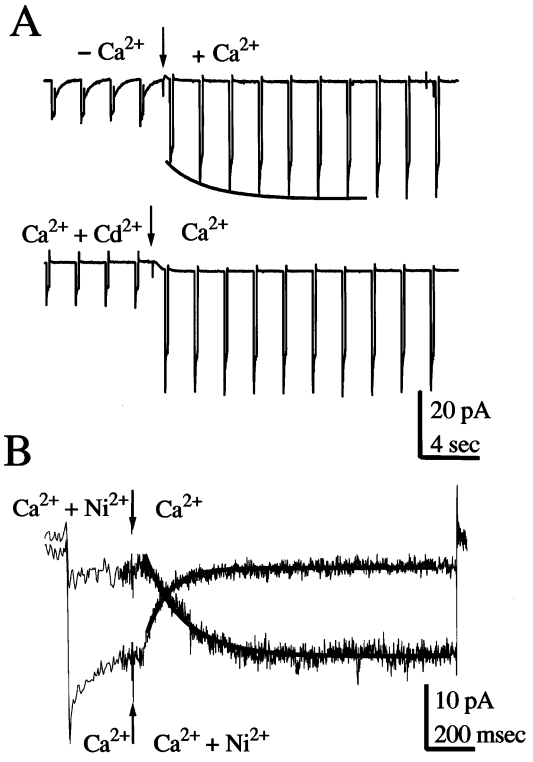

Fig. 7. Lack of effect of inorganic I_{crac} blockers on the Ca^{2+}-dependent enhanced I_{crac} level. Data were obtained from two different cells. (*A*) Whole cell currents (filtered at 30 Hz, digitized at 100 Hz) obtained during a voltage clamp protocol that delivered –100 mV, 200-msec steps at 0.5 Hz from a 0 mV holding potential. In the upper panel, 2 mM Ca^{2+} was reintroduced in place of Ca^{2+}-free solution, resulting in a time-dependent I_{crac} increase. Unbroken line is a monoexponential fit (τ = 2.8 sec) to the current peaks during steps immediately after Ca^{2+} reintroduction. In the lower panel, extracellular solution initially contained 2 mM Ca^{2+} and 1 mM Cd^{2+} resulting in I_{crac} block. An exchange was then made to Cd^{2+}-free solution (arrow), and current reverted rapidly to its full Ca^{2+} permeation level with no time-dependent component evident. (*B*) Superimposed whole cell currents (filtered at 1 kHz, digitized at 5 kHz) in response to –100 mV, 1.5 sec steps (0 mV holding potential). A solution exchange (arrows) entailing either the introduction or removal of 5 mM Ni^{2+} was instituted 250 msec after step onset. All solutions contained 2 mM Ca^{2+}. In the trace associated with upper arrow, extracellular buffer initially contained 5 mM Ni^{2+}, blocking I_{crac} to leak current level. Introduction of Ni^{2+}-free solution resulted in the rapid reappearance of full I_{crac} with no time-dependent component evident. Unbroken line is a monoexponential fit to the data (τ = 171 msec). Trace associated with lower arrow shows that introduction of 5 mM Ni^{2+} instantaneously blocked I_{crac} to leak current level (τ = 85 msec).

al., 1994). It was reasoned that a slow increase in I_{crac} reappearance should be regenerated by instituting a transient block with these cations, if the block interfered with Ca^{2+} reaching its effector site. Neither Ni^{2+} or Cd^{2+} produced this effect (Fig. 7). Current was rapidly blocked to a steady-state basal leak level by either 5 mM Ni^{2+} or 1 mM Cd^{2+}. However, removal of either blocker was accompanied by an apparently instantaneous recovery of I_{crac} to its full preblock amplitude (Ni^{2+}, n = 4; Cd^{2+}, n = 4). Thus blocking Ca^{2+} flux through I_{crac} with these divalents failed to revert I_{crac} to a Ca^{2+}-independent smaller current level, consistent with a site of Ca^{2+} action external to the blocking site.

Discussion

Studies on the regulation of depletion-activated Ca^{2+} currents have focused on biochemical mechanisms, particularly those implicated in coupling microsomal Ca^{2+} store depletion to current activation (*see* Felder, Singer-Lahat & Mathes, 1994, for review). The present report, to our knowledge, is the first to characterize an intrinsic property of I_{crac} whereby Ca^{2+} directly and selectively *enhances* current flux. The major significance of these findings is that they impart an additional characteristic to the biophysical ''fingerprint'' of I_{crac}, that can be subsequently used in comparisons to other depletion-activated channels.

Petersen and Berridge (1994) have reported supralinear increases in depletion-activated Ca^{2+} influx in *Xenopus* oocytes during Ca^{2+} readmission or membrane hyperpolarization. A positive feedback action of Ca^{2+} on the influx pathway was postulated to explain these observations. Whether those reported effects and the Ca^{2+}-dependent I_{crac} increases shown here are due to similar mechanisms is unclear. Possibly, positive feedback by Ca^{2+} on channel activity may be a more generalized property of depletion-activated Ca^{2+} currents. Moreover, if Ca^{2+}-mediated increases are exhibited by Ca^{2+}-selective depletion activated currents that have been recorded successfully at the single channel level (Lückhoff & Clapham, 1994; Vaca & Kunze, 1994), it would prove particularly useful for characterizing this process further: single-channel recordings could ascertain details about the nature of the channel transition (e.g., open probability *vs.* conductance state change; *see below*), as well as its role in determining high Ca^{2+} selectivity of the channel.

Permeation Selectivity of I_{crac}

Ca^{2+} to Ba^{2+} exchanges produced a complex sequence of effects on I_{crac}, which provided insights into permeation and ionic selectivity mechanisms. First, the transient appearance of a current minimum immediately following exchange to Ba^{2+} (Fig. 5, lower panel) was compatible with an anomalous mole fraction effect, brought about by a decrease in Ca^{2+} concentration and concurrent increase in Ba^{2+} concentration at the mouth of the channel. Hoth (1995) recently demonstrated anomalous mole fraction behavior of the Jurkat cell I_{crac} using a series of Ca^{2+}/Ba^{2+} mixtures. Interestingly, the effect was voltage-dependent, becoming prominent at potentials hyperpo-

larized to ~−80 mV. A transient current minimum, analogous to that which we observed, was also shown during Ca^{2+} to Ba^{2+} exchanges at hyperpolarized potentials. Hoth (1995) attributed this to anomalous mole fraction behavior, since it followed the mole-fraction curve generated with the discrete series of Ca^{2+}/Ba^{2+} mixtures.

Importantly, the Ca^{2+}-Ba^{2+} exchange experiments also provided an insight to mechanisms underlying the high Ca^{2+} selectivity of I_{crac}. Ca^{2+} to Ba^{2+} exchanges and those in the reverse order produced, respectively, time-dependent decreases and increases in I_{crac} (Fig. 5), compatible with a reversible transition between a Ca^{2+}-dependent, and a Ca^{2+}-independent state. Hoth (1995) also recently noted a slow time-dependent decrease in I_{crac} following Ca^{2+} to Ba^{2+} exchange with a time course that appears severalfold slower (i.e., 50 to >100 sec to reach steady-state) than that measured in our study ($\tau \sim$ 3.5 sec; *see* Results). Possible differences in experimental conditions that may account for this discrepancy (e.g., solution exchange rates) are unclear. In any event, the findings together support a notion that the high Ca^{2+} selectivity previously described as a hallmark feature of I_{crac} in Jurkat cells (McDonald et al., 1993; Zweifach & Lewis, 1993; Premack et al., 1994) may be conferred by a slow transition in its functional state promoted by the presence of Ca^{2+} at either an extracellular site or within the channel pore.

Mechanism of Ca^{2+}-Dependent I_{crac} Increase

Our evidence argued against an intracellular mechanism for Ca^{2+} action, based on the findings that the strong intracellular buffering conditions, and particularly the rapid Ca^{2+} chelator, BAPTA (Tsien, 1980), did not prevent or alter the effect (Fig. 6). The failure of temporary I_{crac} block by divalent cations in the presence of Ca^{2+} to regenerate the Ca^{2+}-mediated slow I_{crac} reappearance (Fig. 7) also argued against an intracellular site of Ca^{2+} action. Thus, we believe it highly unlikely that the Ca^{2+}-dependent augmentation of I_{crac} was secondary to modulation of an intracellular Ca^{2+}-sensitive biochemical pathway (e.g., phospholipase C), or to a mechanism such as Ca^{2+}-induced Ca^{2+} release from inositol triphosphate (IP_3)-sensitive Ca^{2+} stores, which has been reported to interact with depletion-activated Ca^{2+} influx in *Xenopus* oocytes (Yao & Parker, 1993).

Our experiments did not distinguish whether the Ca^{2+}-induced increase in I_{crac} was mediated extracellularly or from within the channel pore. In either case, the increase in I_{crac} could be explained most parsimoniously by a Ca^{2+}-dependent increase in either open probability or in unitary channel conductance. These possibilities would only be distinguished at the whole cell level by a difficult noise analysis protocol. Single channel analysis of I_{crac} in T lymphocytes is precluded by an extremely low single channel conductance (Zweifach & Lewis, 1993).

Our observations about the constancy of fast inactivation during slow I_{crac} redevelopment (Fig. 2*B*), coupled with previous knowledge about this inactivation process do, however, suggest that a gating mechanism rather than unitary conductance change subserved the Ca^{2+}-mediated I_{crac} increase. The extent of fast inactivation is known to become greater with increasing extracellular Ca^{2+} concentration, a property that has been attributed specifically to augmented Ca^{2+} current strength through unitary I_{crac} channels (Zweifach & Lewis, 1995). Thus, if the slow reappearance of I_{crac} reflected a Ca^{2+}-dependent change in unitary conductance, the extent of fast inactivation would also be expected to increase. Conversely, a Ca^{2+}-dependent increase in open probability would not produce greater unitary channel current strength. Thus the constancy of fast inactivation that was observed here (Fig. 2*B*) would favor an effect on the gating mechanism.

Channel Activation by the Permeant Ion: Diverse Mechanisms?

The augmentation of I_{crac} by Ca^{2+} can be categorized with several other known examples as a general process whereby a permeant ion interacts with a channel to augment current flux. However, the mechanistic similarities among these processes is unclear. Perhaps the best recognized example in this generalized category of effects is associated with microsomal Ca^{2+}-induced Ca^{2+} release via the ryanodine receptor-channel complex. There cytosolic Ca^{2+} itself is capable of activating or enhancing Ca^{2+} flux (Lai & Meissner, 1989). Moreover, the Ca^{2+}-dependent enhancement is due to a direct interaction of Ca^{2+} that increases activation gating (Chen et al., 1993), and the molecular binding site through which Ca^{2+} mediates this effect has been identified (Chen, Zhang & MacLennan, 1993). Cytosolic Ca^{2+} also potentiates Ca^{2+} flux via the IP_3 receptor-channel complex (Iino, 1990; Finch, Turner & Goldin, 1991), but this may differ fundamentally from the ryanodine receptor mechanism: a direct action for Ca^{2+} has not been well established, and the process appears to involve Ca^{2+}-mediated modulation of IP_3 affinity or efficacy. One notable difference between Ca^{2+}-dependent facilitation of either the ryanodine- or IP_3-gated channel activity and the Ca^{2+}-dependent enhancement of I_{crac} is the apparent site of Ca^{2+} action. Cytosolic Ca^{2+}, which exerts these effects on the microsomal channels corresponds to cytosolic Ca^{2+} relative to the I_{crac} channel. Our evidence argues that Ca^{2+}-mediated increases in I_{crac} are not mediated intracellularly.

With regard to plasmalemmal ion channels, Pusch et

al. (1995) recently showed that permeant anions act as a gating charge that induce activation of ClC-0 type Cl^- channels. Varied permeant anion species promoted activation gating of this Cl^- channel with a rank order of selectivity that corresponded precisely to their selectivity order for conductance. The correspondence in selectivities was taken to reflect that activation was mediated by the anions binding at a deep pore site, and accessibility to this site was determined by the intrinsic conductance properties of the pore for each anion (Pusch et al., 1995). By contrast, we found that *only* Ca^{2+} and not other permeant ions (Ba^{2+} or Sr^{2+}) brought about measurable time-dependent increases in I_{crac}. In conclusion, further studies should address whether the Ca^{2+}-dependent enhancement of I_{crac} is subserved by a unique mechanism relative to these other examples of ion channel facilitation by permeant ions.

Note added in proof: After submission of this revised manuscript, we received an *in press* book chapter from Lewis, Dolmetsch and Zweifach (1996) containing some observations similar to those described here.

References

Barry, P.H., Lynch, J.W. 1991. Liquid junction potentials and small cell effects in patch clamp analysis. *J. Membrane Biol.* **121:**101–117

Chad, J.E., Eckert, R. 1984. Calcium domains associated with individual channels can account for anomalous voltage relations of Ca-dependent responses. *Biophys. J.* **45:**993–999

Chen, S.R.W., Vaughan, D.M., Airey, J.A., Coronado, R., MacLennan, D.H. 1993. Functional expression of cDNA encoding the Ca^{2+} release channel (ryanodine receptor) of rabbit skeletal muscle sarcoplasmic reticulum in COS-1 cells. *Biochemistry* **32:**3743–3753

Chen, S.R.W., Zhang, L., MacLennan, D.H. 1993. Antibodies as probes for Ca^{2+} activation sites on the Ca^{2+} release channel (ryanodine receptor) of rabbit skeletal muscle sarcoplasmic reticulum. *J. Biol. Chem.* **268:**13414–13421

Felder, C.C., Singer-Lahat, D., Mathes, C. 1994. Voltage-independent calcium channels. Regulation by receptors and intracellular Ca^{2+} stores. *Biochem. Pharmacol.* **48:**1997–2004

Finch, E.A., Turner, T.J., Goldin, S.M. 1991. Calcium as coagonist of inositol 1,4,5-trisphosphate-induced calcium release. *Science* **252:**443–446

Hamill, O.P., Marty, A., Neher, E., Sakmann, B., Sigworth, F.J. 1981. Improved patch-clamp techniques for high-resolution recording from cells and cell-free membrane patches. *Pfluegers Arch.* **391:**85–100

Hardie, R.C., Minke, B. 1993. Novel Ca^{2+} channels underlying transduction in Drosophila photoreceptors: implications for phosphoinositide-mediated Ca^{2+} mobilization. *TINS* **16:**371–376

Hoth, M. 1995. Calcium and barium permeation through calcium release-activated (CRAC) channels. *Pfluegers Arch.* **430:**316–322

Hoth, M., Penner, R. 1992. Depletion of intracellular calcium stores activates a calcium current in mast cells. *Nature* **355:**353–356

Hoth, M., Penner, R. 1993. Calcium release-activated calcium current in mast cells. *J. Physiol.* **465:**359–386

Iino, M. 1990. Biphasic Ca^{2+} dependence of inositol 1,4,5-trisphosphate-induced Ca^{2+} release in smooth muscle cells of the guinea pig *taenia caeci. J. Gen. Physiol.* **95:**1103–1122

Lai, F.A., Meissner, G. 1989. The muscle ryanodine receptor and its intrinsic Ca^{2+} channel activity. *J. Bioenerg. Biomembr.* **21:**227–246

Lewis, R.S., Cahalan, M.D. 1989. Mitogen-induced oscillations of cytosolic Ca^{2+} and transmembrane Ca^{2+} current in human leukemic T cells. *Cell Regulation* **1:**99–112

Lewis, R.S., Dolmetsch, R.E., Zweifach, A. 1996. Positive and negative regulation of depletion-activated calcium channels by calcium. *In:* Organellar for Channels and Transporters. D.E. Clapham and B.E. Ehrlich, editors. Rockefeller University Press, New York (*in press*)

Lückhoff, A., Clapham, D.E. 1994. Calcium channels activated by depletion of internal calcium stores in A431 cells. *Biophys. J.* **67:**177–182

McDonald, T.V., Premack, B.A., Gardner, P. 1993. Flash photolysis of caged inositol 1,4,5-trisphosphate activates plasma membrane calcium current in human T cells. *J. Biol. Chem.* **268:**3889–3896

Petersen, C.C.H., Berridge, M.J. 1994. The regulation of capacitative calcium entry by calcium and protein kinase C in *Xenopus* oocytes. *J. Biol. Chem.* **269:**32246–32253

Premack, B.A., McDonald, T.V., Gardner, P. 1994. Activation of Ca^{2+} current in Jurkat T cells following the depletion of Ca^{2+} stores by microsomal Ca^{2+}-ATPase inhibitors. *J. Immunol.* **152:**5226–5240

Pusch, M., Ludewig, U., Rehfeldt, A., Jentsch, T.J. 1995. Gating of the voltage-dependent chloride channel ClC-0 by the permeant anion. *Nature* **373:**527–531

Tsien, R.Y. 1980. New calcium indicators and buffers with high selectivity against magnesium and protons: design, synthesis and properties of prototype structures. *Biochemistry* **19:**2396–2404

Vaca, L., Kunze, D.L. 1994. Depletion of intracellular Ca^{2+} stores activates a Ca^{2+}-selective channel in vascular endothelium. *Am. J. Physiol.* **267:**C920–C925

Vaca, L., Sinkins, W.G., Hu, Y., Kunze, D.L., Schilling, W.P. 1994. Activation of recombinant *trp* by thapsigargan in Sf9 insect cells. *Am. J. Physiol.* **267:**C1501–C1505

Yao, Y., Parker, I. 1993. Inositol triphosphate-mediated Ca^{2+} influx into *Xenopus* oocytes triggers Ca^{2+} liberation from intracellular stores. *J. Physiol.* **468:**275–296

Zweifach, A., Lewis, R.S. 1993. Mitogen-regulated Ca^{2+} current of T lymphocytes is activated by depletion of intracellular Ca^{2+} stores. *P.N.A.S.* **90:**6295–6299

Zweifach, A., Lewis, R.S. 1995. Rapid inactivation of depletion-activated calcium current (I_{crac}) due to local calcium feedback. *J. Gen. Physiol.* **105:**209–226